HHS Public Access

Author manuscript

Nanomedicine. Author manuscript; available in PMC 2023 January 01.

Published in final edited form as:

Nanomedicine. 2023 January ; 47: 102614. doi:10.1016/j.nano.2022.102614.

Monophosphoryl lipid A-adjuvanted nucleoprotein-neuraminidase nanoparticles improve immune protection against divergent influenza viruses

Ye Wang[1,†], **Chunhong Dong**[1,†], **Yao Ma**[1], **Wandi Zhu**[1], **Harvinder Singh Gill**[2], **Timothy L. Denning**[1], **Sang-Moo Kang**[1], **Bao-Zhong Wang**[1,*]

[1]Center for Inflammation, Immunity & Infection, Georgia State University Institute for Biomedical Sciences, 100 Piedmont Ave SE, Atlanta, Georgia 30303, USA

[2]Department of Chemical Engineering, Texas Tech University, Lubbock, TX 79409, USA

Abstract

Universal influenza vaccines are urgently needed to prevent recurrent influenza epidemics and inevitable pandemics. We generated double-layered protein nanoparticles incorporating two conserved influenza antigens—nucleoprotein and neuraminidase—through a two-step desolvation-crosslinking method. These protein nanoparticles displayed immunostimulatory properties to antigen-presenting cells by promoting inflammatory cytokine (IL-6 and TNF-α) secretion from JAWS II dendric cells. The nanoparticle immunization induced significant antigen-specific humoral and cellular responses, including antigen-binding and neutralizing antibodies, antibody- and cytokine (IFN-γ and IL-4)-secreting cells, and $NP_{147–155}$ tetramer-specific cytotoxic T lymphocyte (CTL) responses. Co-administration of monophosphoryl lipid A (MPLA, a toll-like receptor 4 agonist) with the protein nanoparticles further improved immune responses and conferred heterologous and heterosubtypic influenza protection. The MPLA-adjuvanted nanoparticles reduced lung inflammation post-infection. The results demonstrated that the combination of MPLA and conserved protein nanoparticles could be developed into an improved universal influenza vaccine strategy.

Keywords

MPLA; nucleoprotein; neuraminidase; protein nanoparticle; universal influenza vaccine

[*]**Correspondence:** Bao-Zhong Wang, Tel: (1)-404-413-3652; Fax: 404-413-3580, bwang23@gsu.edu.

[†]These authors have contributed equally to this work and share the first authorship.

Author contributions

Ye Wang, Bao-Zhong Wang: Conceptualization. Ye Wang, Chunhong Dong, Yao Ma, Wandi Zhu: Investigation, Methodology, Data Analysis. Ye Wang, Chunhong Dong: Writing- Original draft preparation, Reviewing and Editing. Harvinder Singh Gill, Timothy L. Denning, Sang-Moo Kang, Bao-Zhong Wang: Funding acquisition, Project administration, Resources, Supervision, Writing - review & editing.

Conflict of interest: All authors have declared no financial or other potential conflicts of interest.

Introduction

Seasonal influenza vaccination is the most cost-effective strategy to combat influenza. However, current influenza vaccines mainly target the variable hemagglutinin (HA), can only provide robust strain-specific immunity, and show low efficiency against mutated seasonal and pandemic influenza strains [1]. In 2018, the National Institute of Allergy and Infectious Diseases (NIAID) unveiled its strategic plan for developing a universal influenza vaccine that targets conserved influenza epitopes and provides durable cross-protection against multiple influenza strains [2]. Since then, scientists have made extensive efforts to develop cross-protective influenza vaccines by including more conserved, mutation-resistant antigens. Promising results have been achieved by applying the HA stalk domain [3, 4], matrix protein 2 ectodomain (M2e) [5], neuraminidase (NA) [6, 7], or nucleoprotein (NP) [8] in vaccine formulations.

NA is the second most abundant influenza surface glycoprotein and contributes to the release of new virions from infected cells. Compare with HA, NA has a relatively slower antigenic drift rate [9]. Because antigenic mutation of NA occurs independently of HA, NA-specific antibodies may help prevent variant strains in which HA but not NA changes [10]. The highly conserved epitope $NA_{222–230}$ has elicited universal anti-NA antibodies against all subtypes of influenza A [11]. $NA_{222–230}$ and $NA_{275–281}$ were fused to the HA head domain and combined with Army liposomal adjuvant (ALFQ) for broader influenza immunity. Both approaches induced broadly neutralizing NA-specific antibodies [12, 13]. So far, eleven NA subtypes have been identified for influenza A viruses IAVs [14]. With IAVs H1N1 and H3N2 causing most epidemic diseases in humans, N1 and N2 become promising immune targets for vaccine development.

NP is the most abundant influenza protein, supporting the structure of the vRNP complex during viral replication within the influenza virion, and is relatively conserved among all influenza A subtypes [15]. NP is a potent inducer of broadly reactive cytotoxic T lymphocyte (CTL) responses. Inclusion of the conserved epitope $NP_{147–155}$ in an influenza vaccine candidate resulted in robust CTL immune responses and quicker viral clearance [8, 16]. However, the conserved epitopes generally suffer from low immunogenicity.

Nanotechnology provides a promising and innovative platform for vaccine development. Various nanoparticles have demonstrated intriguing advantages, including virus-mimetic nanoscale size, repetitive antigen presentation, controlled antigen release, good stability, targeted antigen delivery, and intrinsic immune-stimulating properties [17–19]. Moreover, nanoparticle platforms may facilitate logistically simplified and rapid vaccine manufacturing, cold-chain independent storage and distribution, and mass administration, resulting in affordable vaccine development [20, 21]. Desolvation-driven protein nanoparticles containing pure antigen composition are a promising vaccine platform because of their biocompatibility and high safety [22, 23]. Moreover, the protein nanoparticles serve as antigen reservoirs, boosting antigen immunogenicity [8]. Previously, we demonstrated that double-layered protein nanoparticles containing M2e and HA stalk or NA induced robust cross-protective antibodies [4, 6].

Adjuvants can trigger early and proper innate immune responses locally to aid in the generation of robust and long-lasting adaptive immune responses in multiple ways, including modulating cytokine and chemokine production, recruiting and activating immune cells, and enhancing antigen uptake, processing, and presentation by antigen-presenting cells (APCs) [24, 25]. Monophosphoryl lipid A (MPLA), a detoxified low-toxicity derivative of the lipid A region of bacterial lipopolysaccharide (LPS), is a well-known potent adjuvant to enhance immune responses against virus infection [26]. While the toxicity associated with LPS prohibits its potential clinical use, MPLA is being developed as a vaccine adjuvant [27]. MPLA activates the toll-like receptor 4 (TLR4) signal pathway, resulting in enhanced type I IFN production but diminished inflammatory cytokines [28, 29]. MPLA has been included in licensed adjuvant combinations, such as AS04 (MPL and Alum, for hepatitis B virus and human papillomavirus) and AS01 (MPL, saponin QS21, and CpG1018, for herpes zoster and HBV vaccines), to induce comprehensive immune responses to vaccine antigens [30]. The inclusion of MPLA promoted antigen uptake by APCs [31] and facilitated the maturation of dendric cells, leading to augmented antigen-specific CD8+ T lymphocyte responses [32] and germinal center responses [33].

We fabricated novel influenza NP and NA protein nanoparticles in this study using a two-step desolvation-crosslinking method [4]. We systematically characterized the nanoparticles and investigated the nanoparticle-induced antigen-specific humoral and cellular responses with or without co-administration of MPLA. We performed challenge studies with homologous, heterologous, and heterosubtypic viruses. Our results indicated that the MPLA-adjuvanted nanoparticle group protected mice against different influenza viruses.

Results

Fabrication and characterization of double-layered NP-NA (core-shell) nanoparticles

We generated recombinant baculoviruses (rBVs) to produce NP, as shown in Figure S1A. Recombinant NP was purified from Sf9 insect cells. The protein shows a single clean band with expected molecular weight. We also purified NA1 and NA2 fusion proteins (Figure S1B) as described previously [7].

NP protein nanoparticles were prepared by ethanol desolvation of NP solution. We generated layered NP-NA (core-shell) protein nanoparticles by crosslinking NA1 (N1) or NA2 (N2) onto the surface of NP protein nanoparticle cores (Figure 1A). The Coomassie Blue staining and Western Blotting analysis demonstrated the composition of the layered protein nanoparticles (Figures 1B and 1C). NP and N1 showed similar bands location in the SDS-PAGE gel. The ratio of NA2 to NP was around 1:4, determined by the GelQuantNET software. The resulting NP nanoparticle cores were 211.3+/−18.6 nm in diameter (Figure 1D). The layered NP-N1 and NP-N2 protein nanoparticles were 253.3 +/− 23.5 nm and 245.6 +/− 28.7 nm in diameters, respectively. NP-N1 and NP-N2 showed negative ζ-potentials of −33.54 +/− 0.58mV and −32.76 +/−0.97 mV (Figure S1C), respectively. Scanning electron microscope (SEM) images revealed a roughly spherical shape of the layered protein nanoparticles (Figure S1D).

We further evaluated whether the resulting protein nanoparticles could stimulate the APCs by examining the production of inflammatory cytokines, interleukin 6 (IL-6) and tumor necrosis factor α (TNF-α), from JAWS II dendritic cells (DCs). Compared with soluble protein treatment groups, both NP-N1 and NP-N2 nanoparticles significantly elevated IL-6 and TNF-α production (Figure 1E).

MPLA-adjuvanted nanoparticles increased antigen-specific immune responses

To further improve vaccine efficiency, we combined a mixture of the NP-N1 and NP-N2 protein nanoparticles (NP-N1/N2) with MPLA. Three weeks after the boosting immunization, the MPLA-adjuvanted nanoparticle groups (NP-N1/N2 + MPLA) showed significantly higher N1- or N2-specific binding antibody levels in immune sera than those without MPLA (Figure 2A). The NP-N1/N2 + MPLA immune sera showed potent neutralization against both homologous and heterologous NA influenza strains, consistent with our previous studies [6, 7], but a low neutralizing activity against a heterosubtypic H7N9 virus (Figure 2B). Further analysis of NA-specific IgG isotype (IgG1 and IgG2a) indicated that although all nanoparticle-immunized mice produced more IgG1 than IgG2a, a more balanced IgG2a/IgG1 ratio was observed in MPLA-adjuvanted group (Figure 2C). The NP-N1/N2 + MPLA immunization group also generated more NA (N1 or N2)-specific antibody-secreting cells than that without MPLA in the bone marrow from the immunized mice (Figure 2D).

We detected cytokine-secreting splenocytes under antigen re-stimulation by ELISpot assay to evaluate the NA-specific cellular immune responses. A significantly increased number of interferon-gamma (IFN-γ) or interleukin-4 (IL-4)-secreting splenocytes was observed in the NP-N1/N2 + MPLA groups (Figures 2E–F).

We also evaluated NP-specific cellular immune response three weeks post-boosting immunization by flow cytometry and ELISpot assays. As shown in Figures 3A and 3B, all the nanoparticle groups (NP core, NP-N1/N2, or NP-N1/N2 + MPLA) boosted significantly increased $NP_{147–155}$ (a CTL epitope [34]) tetramer-positive CD8 ($NP_{147–155}$ tetramer^{+}CD8^{+}) T cells in mouse spleens than the control group). In addition, NP-N1/N2 + MPLA immunization generated more IFN-γ- and IL-4-secreting splenocytes than the NP-N1/N2 group (Figure 3C).

MPLA-adjuvanted nanoparticle immunization protected mice against various influenza virus challenges

After confirming the robust NA-specific immune response induction by NP-NA nanoparticles, we tested whether the combined NP-N1/N2 nanoparticle immunization could protect mice against homologous reassortant A/Vietnam/1203/2004 (rViet, H5N1) and A/Aichi/2/1968 (Aichi, H3N2) viruses. In a challenge study, we found that NP-N1/N2 and NP-N1/N2 + MPLA groups maintained 100% survival rates (Figures 4A and B). The NP-N1/N2 + MPLA groups showed less bodyweight loss than the NP-N1/N2 groups.

To examine the protection against heterologous influenza viruses, we immunized mouse groups with N1 nanoparticles (NP-N1, NP-N1/N2, and NP-N1/N2 + MPLA) and challenged them with A/Puerto Rico/8/34 (PR8, H1N1). Previously we have found that N1 (from

H5N1 influenza virus)-specific immune sera could protect mice against heterogenous PR8 challenge [6]. As shown in Figure 4C, the NP core nanoparticle (NP Nano) group showed the most bodyweight loss and a 50% survival rate. In comparison, all the N1-containing nanoparticle groups demonstrated 100% survival rates. The NP-N1/N2 + MPLA group maintained the most negligible body weight loss. These results suggested that co-administration of MPLA improved the protection efficiency of the protein nanoparticles against homologous and heterologous influenza strains in mice.

We challenged the N2 nanoparticle group set (NP-N2, NP-N1/N2, and NP-N1/N2 + MPLA) with a reassortant A/Shanghai/2/2013 (rSH, H7N9) influenza virus to examine the protection against the heterosubtypic influenza virus. The NP Nano group showed no protection (0% survival rate). The NP-N2 and NP-N1/N2 groups had 25% survival rates, while the NP-N1/N2 + MPLA groups showed 50% survival rates (Figure 4D). Nevertheless, no significant difference was observed between NP-N1/N2 vs NP-N1/N2+MPLA vaccination against H7N9 protection.

MPLA-adjuvanted nanoparticle immunization reduced lung inflammation and virus replication post-infection

We collected mouse lungs five days post-infection for histological examination and viral load detection. As shown in Figure 5, naïve mice suffered from severe lung inflammation and high viral loads post-infection. NP Nano immunization showed limited protection. Among all the groups, the MPLA-adjuvanted NP-N1/N2 groups displayed the least alveolar inflammatory infiltration, tissue damage, and viral loads upon the infection by H5N1 or H3N2. The NP-N1/N2 groups had inflammation and viral loads at a middle level.

NP has been recognized as the primary target for T cell-based universal influenza vaccine development. We incorporated NP inside our double-layered nanoparticles to induce NP-specific cytotoxic T-lymphocytes (CTL) responses. We investigated the numbers of $NP_{147–155}$ tetramer-positive CTL in the draining mediastinal lymph nodes (MLNs) 5 days post-infection with 1× LD_{50} of H3N2. As shown in Figure 6, the NP-containing nanoparticles significantly increased $NP_{147–155}$ tetramer-positive CD8 T cell responses in MLNs compared with the naïve mice. The NP-N1/N2 + MPLA groups induced the most $NP_{147–155}$ tetramer-positive CD8+ T cell responses. Therefore, despite the limited protection conferred by NP Nano, the NP in these nanoparticles induced strong CTL immune responses upon virus infection.

Discussion

Influenza poses significant health and economic risk, circulates annually, and occasionally causes pandemics [35]. Influenza replicates its genome with error-prone RNA polymerases and experiences high antigenic shift and drift rates, resulting in the current influenza vaccines' low efficacy [36]. Therefore, a universal influenza vaccine with conserved antigens that can offer cross-protection is needed to combat moving influenza targets and thwart the emergence of novel influenza pandemics [37].

Desolvation-driven protein nanoparticles have many immunological and logistical advantages [37, 38]. Most proteins can be precipitated using desolvation reagents such as neutral salts or organic solvents (methanol, ethanol, etc.) in a scalable manufacturing process [39]. The particle size is tunable, depending on the volume of desolvation reagents, the type of desolvation reagents, and the stirring speed during the process [38, 40]. The method of coating protein cores with protein shells enables customizable antigen combinations and broadens the antigen pool for vaccine development. Compared with most other particulate vaccine platforms, the protein nanoparticle platform composes solely of antigenic proteins/peptides of interest, avoiding unfavorable off-target carrier-specific side effects and ensuring high safety profiles. Moreover, protein nanoparticles displayed other advantageous features over soluble proteins, including focused size distribution, improved antigen stability, controlled antigen release, as well as immunostimulatory effects. The protein nanoparticles in our study promoted the inflammatory cytokine (IL-6 and TNF-α) secretion from JAWS II DCs.

Previously, we desolvated M2e into nanoparticles as the inner core of double-layered protein nanoparticles. M2e inner cores have been used in several layered nanocluster fabrications along with influenza surface antigen-derived recombinant proteins in the outer layers, including the full-length HA, head removed HA, and M2e-NA fusion protein [4, 6, 41]. This study applied NP as the core protein to induce NP-specific T cell responses. The epitopes from NP are highly conserved across influenza viruses. Researchers have utilized these conserved NP-related epitopes in adenoviral vector-based vaccine candidates [42]. We observed that NP-containing nanoparticle groups induced a robust $NP_{147–155}$ tetramer-specific CTL immune response, even in the uncoated NP core group. However, the NP Nano group had a suboptimal 50% survival rate against H1N1 and no protection against H7N9. Our results were consistent with previous studies where an $NP_{147–155}$ tetramer-based recombinant adenovirus induced a strong CTL immune response but did not decrease the viral titer nor protect mice against challenges by PR8 (H1N1) [34]. Therefore, the single antigen NP nano could provide limited protection against lethal influenza challenges.

We fabricated double-layered protein nanoparticles by conjugating NA protein around NP core surfaces, mimicking the native viral presentation, synergizing with the NP-induced immune responses to improve the protection against influenza challenges. The NA within such nanoparticles generated more protective neutralizing antibodies and antibody-secreting cells and improved the protection against homologous H5N1, H3N2, or heterologous H1N1.

A co-administration of MPLA with protein nanoparticles significantly boosted the antigen-specific immune responses. We observed significantly increased and more balanced antigen-binding and neutralizing antibodies, and antibody-secreting cells in bone marrow in the MPLA-adjuvanted groups. Vaccine-induced IgG isotypes play divergent but important roles in combating influenza infection [19, 43]. Th2-type IgG1 mainly associates with virus neutralization, the main contributor to protection against homologous or closely virus strains but may not work against distantly related strains. In comparison, murine Th1-type IgG2a —with the greatest ability to activate Fc receptor-mediated effector responses among all IgG isotypes— correlates with the virus clearance from infected hosts, improving cross-

protection in the absence of cross-neutralizing antibodies. The MPLA plays an important role in boosting the diversified anti-NA antibodies with a more balanced IgG2a/IgG1 ratio.

We also observed that the addition of MPLA boosted the IL-4 and IFN-γ-secreting cells production. IL-4 is the dominant Th2 deviator for initiating and expanding humoral immunity [44]. IL-4 derived from follicular helper T cells has an essential role in developing germinal center B cells [45]. The high IL-4-secreting lymphocytes observed were consistent with the boosted antibody responses. IFN-γ, a typical Th1-type cytokine, also plays multiple essential roles in the induction of protective cellular immune responses against influenza [46]. An increased survival rate indicated that the combination with MPLA adjuvant broadened and improved such protection. The MPLA-adjuvanted group displayed lowered lung inflammation and viral load post-infection. In summary, the MPLA-adjuvanted NP-N1/N2 nanoparticles induced improved humoral and CTL immune responses, conferring the best protection against homologous, heterologous, or heterosubtypic influenza challenges among all the groups in our study.

However, we found that the NP-NA nanoparticle vaccines only provided modest heterosubtypic protection even in the presence of MPLA, which was probably due to the inherent relatively weak heterosubtypic protection of these antigens. Our current results are consistent with previous studies that implicated that conserved influenza antigens like NP and NA may not be sufficient for providing optimal universal influenza protection [6, 34]. Some studies also indicated the ability of an NP-based vaccine to provide protection at higher antigen doses up to 100 μg and/or multiple vaccinations [47, 48]. The protection may be formulation- and dose-dependent. Still, NP and NA-mediated immunity is infection-permissive and not optimal for protecting the hosts against body weight loss and morbidity. Vaccine formulations including multiple potent conserved antigens including head-removed HA (hrHA) and M2e to induce both potent broadly neutralizing antibody and cellular responses could be a promising strategy to develop comprehensively protective universal influenza vaccines. The MPLA-adjuvanted NP-NA protein nanoparticles could be a synergistic piece of the universal influenza vaccine puzzle.

Materials and Methods

Materials

MPLA (MPLA-SM VacciGrade™, Cat. code: vac-mpla) was purchased from Invivo Gen, USA. Peptide pools, including NP (NR-2611), NA1 (NR-19258), or NA2 (NR-2608) were obtained from BEI Resources, USA.

Ethics statement and statistical analysis methods

The work in this study was completed under IACUC protocol A19025 of the Georgia State University Institutional Animal Care and Use Committee (IACUC). A body weight loss > 20% was used as the humane endpoint, at which mice were euthanized per IACUC guidelines. Data were presented by mean +/− standard error of the mean with One-way ANOVA. Tukey's multiple comparison post-test was used for statistical significance

analysis. Log-rank test was used for statistical survival rate analysis. A p-value less than 0.05 ($p < 0.05$) was recognized as significant.

Preparation of the recombinant proteins and protein nanoparticles

The construction of the NP protein-encoding gene (*np*) and tetrameric NA fusion protein-encoding gene (*na*) was done as previously described [7]. Briefly, a honeybee melittin signal peptide (melittin), a hexahistidine-tag (his-tag), and NP fusion protein-encoding sequences (*np*) were fused in the open reading frame and subcloned into the transfer vector pFastBac for recombinant baculovirus (rBV) generation. We adapted the same NA fusion protein-encoding gene (*na*) as previously described [7]. Full-length NP protein was from A/Puerto Rico/8/1934 (PR8, H1N1, GenBank: ABD77679.1, 1M to 498N). The NA1 ectodomain was from A/Vietnam/1203/2004 (Viet, H5N1, Genbank: EF541467, 36H to 449K), and the NA2 ectodomain was from A/Aichi/2/1968 (Aichi, H3N2, Genbank: AB295606, 38K to 469I). According to their separate amino acid sequence, the estimated molecular weight for NP, NA1, and NA2 was 57.2, 52.9, and 56.2 kDa, respectively. However, the final NA1 and NA2 showed bands at around 58 and 62 kDa on the sodium dodecyl sulfate–polyacrylamide gel electrophoresis (SDS-PAGE), respectively, owing to protein glycation, as we previously reported [7]. Ni-NTA resin was used to purify the recombinant proteins from insect cell culture supernatants [7].

We fabricated and characterized NP particle cores and double-layered NP-N1 and NP-N2 nanoparticles [6]. Briefly, the NA fusion protein was crosslinked onto the desolvated NP nanoparticle surfaces using a DTSSP crosslinking reaction for 1.5 hours. The nanoparticles were then collected and sonicated for characterization or immunization.

Characterization of the protein nanoparticles

The size and ζ-potentials of the nanoparticles were measured by dynamic light scattering (DLS) analysis with a Malvern Zetasizer Nano ZS. The nanoparticle morphology was visualized by scanning electron microscope (SEM) with a Zeiss LEO 1450vp (Carl Zeiss, Jena, Germany) at 5.0 kV, after being resuspended in water, air-dried, and sputter-coated with carbon. The nanoparticle compositions were confirmed using SDS-PAGE followed by Coomassie blue staining and Western blotting. 10 μL of NP-NA nanoparticles (0.5 μg/μL) was mixed with 10 μL of 5% β-mercaptoethanol, followed by heating at 99 °C for 10 minutes and separation by reduced 1% SDS-PAGE gel. A certain amount of sN1 and sNP were loaded as controls for NP-N1 in Western blotting analysis. The ratio of NA/NP was determined using GelQuantNET software after Coomassie blue staining by comparing the band intensity of NA2 to NP. Anti-his antibodies (Thermo Fisher, MA1-21315) were used as the primary antibody for the Western blotting analysis.

Proinflammatory Cytokine Profiles of Stimulated JAWS II Cells

JAWS II cells were seeded at 4×10^4 cells/well (100 μL/well) into 96-well cell culture plates as previously described [49]. Cells were treated with 5 μg/mL of soluble protein mixtures or NP-NA protein nanoparticles for 16 h. Untreated cells were used as negative controls. Supernatant proinflammatory cytokine (IL-6 and TNF-α) levels were evaluated using cytokine enzyme-linked immunosorbent assay (ELISA) kits (Thermo Scientific, USA).

Immunization and influenza infection

Female BALB/c mice (aged 6–8 weeks) received the primary and boosting intramuscular (i.m.) immunizations on days 0 and 28, respectively, in the hind leg with 50 μl of vaccine mixture in DPBS containing 5 μg of NP-N1, NP-N2, NP-N1/N2 (a formulation comprising a mixture of 2.5 μg of NP-N1 and 2.5 μg of NP-N2) nanoparticles, or soluble protein mixtures (containing the same amount of NP and NA proteins as that in nanoparticles). For MPLA-adjuvanted groups (10 μg per mouse), MPLA was mixed with the vaccine formulations before immunization. 50 μl of DPBS was used as a placebo. Orbital blood was collected from mice anesthetized with 1% isoflurane twenty-one days after the priming and boosting immunization, followed by blood clotting and centrifugation to obtain sera samples.

A set of mice groups were challenged by different influenza viruses (50 μL in saline solution) 28 days after the boost immunization. For the homologous NA group cluster, mice (n=5) were challenged by $5\times LD_{50}$ reassortant Viet (rViet, H5N1) or A/Aichi/2/1968 (Aichi, H3N2) viruses. For the heterologous or heterosubtypic NA group cluster, mice (n=4) were challenged by lethal doses of $3\times LD_{50}$ of A/PR8/1934 (H1N1) or A/Shanghai/2013 (H7N9) viruses. The NA sequence identities between different virus strains were calculated as rViet H5N1 v.s. PR8 H1N1 (GeneBank No. AY651447 for PR8 NA, 84%), rViet H5N1 v.s. rSH H7N9 (GeneBank No. KF021599 for rSH NA, 44%), Aichi H3N2 v.s. PR8 H1N1 (41%), and Aichi H3N2 v.s. rSH H7N9 (45%), respectively. The reassortant A/Vietnam/1203/2004 (rViet, H5N1; HA and neuraminidase (NA) genes derived from Viet, and the remaining backbone genes from PR8) and A/Shanghai/2/2013 (rSH, H7N9; HA and NA genes derived from SH, and the remaining backbone genes from PR8) viruses were generated and rescued as previously described [4]. Mouse body weight loss and final survival rates were recorded for 14 days post-infection.

Another set of nanoparticles (NP nano, NP-N1/N2, or NP-N1/N2 + MPLA)-immunized and naïve mice were infected by 1× LD50 rViet or 1× LD50 Aichi virus, respectively, followed by lung histological examination and lung virus titration five days post-infection. PBS-immunized mice were used as control.

ELISA assay

Antigen (NA1 and NA2)-specific total IgG and IgG subtype (IgG1 and IgG2a) antibody responses were examined by ELISA, as described previously [6]. 50 μL of antigen proteins (4 μg/mL) was used for coating plates at 4 °C overnight. Sera from different groups were incubated in NA1 or NA2-coated plate wells for 2 hours at 37 °C. Goat anti-mouse IgG, IgG1, and IgG2a conjugated with horseradish peroxidase (HRP) (SouthernBiotech, Cat. No.1030-05) was incubated in the wells for another 2 hours at room temperature. 3,3′,5,5′-Tetramethylbenzidine (TMB) and 1 M sulfuric acid were used for developing the colors and stopping the reaction, respectively.

Neuraminidase inhibition (NAI) assay

NAI assay was performed as previously described [7]. Sera were heat-inactivated at 56 °C for 30 minutes. 50 μL of serially 2-fold-diluted sera were mixed with 50 μL of diluted rViet

H5N1, Aichi H3N2, PR8 H1N1, and rSH H7N9 influenza virus solution (8000 TCID50) at 37°C for 30 minutes. The mixtures of serum-virus were incubated in Fetuin-coated plates at 37°C for 2 hours. HRP-conjugated lectin from Arachis hypogaea peanut (Sigma, Cat. No. L6135-1MG) was added and then incubated for 2 h. TMB was used to develop the signal, and the reaction was stopped with 1M sulfuric acid after the incubation of HRP-conjugated lectin.

ELISpot assay

ELISpot was used to evaluate the numbers of antigen (NP, NA1, and NA2)-specific IL-4- or IFN-γ- secreting cells and antibody-secreting cells after three weeks post boosting immunization as previously described [50]. Spleens and bone marrow were collected and processed into single-cell suspensions with complete Roswell Park Memorial Institute (RPMI) 1640 media. 3×10^5 splenocyte or bone marrow single-cell suspensions were seeded onto 96-well filtration plates. For B-cell ELISpot assay, the purified NA1 or NA2 proteins were used for coating the filtration plates to detect the NA1 or NA2-specific antibody-secreting cells, respectively. For T-cell ELISpot assay, a final concentration of 2 μg/mL NP, NA1, or NA2 peptide mixture was used for stimulating the cells. PBS-immunized mouse samples were used as negative controls.

Flow cytometry

PE-conjugated $NP_{147–155}$-specific MHC-I tetramers were synthesized by the Emory University Tetramer Lab. Spleens were collected from different groups of immunized mice for CD8 and $NP_{147–155}$ tetramer positive splenocytes detection. An NP peptide mixture (at a final concentration of 4 μg/mL) was added to homogenized splenocytes for stimulation overnight. The splenocytes were stained by surface marker CD8-PE-Cy5 and $NP_{147–155}$ tetramer-PE. For mediastinal lymph node (MLN) CD8 T cell detection, MLN tissues from different groups were collected 5 days post-infection with 1× LD_{50} of H3N2. The homogenized lymphocytes were stained by surface marker CD8-PE-Cy5 and $NP_{147–155}$ tetramer-PE. BD LSRFortessa™ was used for examining stained cells. Data were analyzed with the FlowJo software application.

Histological analysis and lung virus titration

On day five post-infection, lungs from different groups were harvested, dehydrated, fixed, and embedded in paraffin. Lung sample paraffin sections were stained with hematoxylin and eosin (H&E). Three 10-μm-thick sections from three different parts of the lungs were examined microscopically by three unbiased pathologists. The degree of leukocyte infiltration was scored on a scale of 0 to 4 as described previously [7, 49]. Scores were given as absent (0), subtle (1), mild (2), moderate (3), and severe (4).

For lung virus titration, lung samples were ground with a cell strainer and separated by Percoll gradient centrifugation, as described previously [6]. Madin-Darby canine kidney (MDCK) cells-coated 96-well plates were incubated with 100 μL of serially 10-fold diluted lung supernatants from infected mice. Five days post-incubation, 50 μL of MDCK supernatants were transferred to V-shape 96-well plates and mixed with the same volume

of 0.5% turkey red blood cells. The Reed-München method was used for the calculation of hemagglutinin activity titers.

Supplementary Material

Refer to Web version on PubMed Central for supplementary material.

Acknowledgments

This work was financially supported by the US National Institutes of Health (NIH)/National Institute of Allergy and Infectious Diseases (NIAID) under grants R01AI101047, R01AI116835, and R01AI143844 to B.-Z.W.

Abbreviations

MPLA	monophosphoryl lipid A
CTL	cytotoxic T lymphocyte
HA	hemagglutinin
NIAID	the National Institute of Allergy and Infectious Diseases
M2e	matrix protein 2 ectodomain
NA	neuraminidase
NP	nucleoprotein
APC	antigen-presenting cell
LPS	lipopolysaccharide
TLR4	toll-like receptor 4
rBVs	recombinant baculovirus
SEM	scanning electron microscope
SDS-PAGE	sodium dodecyl sulfate–polyacrylamide gel electrophoresis
DCs	dendritic cell
IFN-γ	interferon-gamma
IL-4	interleukin-4
IL-6	interleukin-6
TNF-α	tumor necrosis factor-α
MLN	mediastinal lymph node
hrHA	head-removed HA
DLS	dynamic light scattering

ELISA	enzyme-linked immunosorbent assay
HRP	horseradish peroxidase
TMB	3,3’,5,5’-Tetramethylbenzidine
NAI	neuraminidase inhibition
RPMI	Roswell Park Memorial Institute
H&E	hematoxylin and eosin
MDCK	Madin-Darby canine kidney

References

1. CDC. 2020–2021 Flu Season Summary. July, 22nd 2021.
2. Erbelding EJ, Post DJ, Stemmy EJ, Roberts PC, Augustine AD, Ferguson S, et al. A Universal Influenza Vaccine: The Strategic Plan for the National Institute of Allergy and Infectious Diseases. J Infect Dis 2018; 218: 347–54. [PubMed: 29506129]
3. Yassine HM, Boyington JC, McTamney PM, Wei CJ, Kanekiyo M, Kong WP, et al. Hemagglutinin-stem nanoparticles generate heterosubtypic influenza protection. Nat Med 2015; 21: 1065–70. [PubMed: 26301691]
4. Deng L, Mohan T, Chang TZ, Gonzalez GX, Wang Y, Kwon YM, et al. Double-layered protein nanoparticles induce broad protection against divergent influenza A viruses. Nat Commun 2018; 9: 359. [PubMed: 29367723]
5. Kim MC, Song JM, O E, Kwon YM, Lee YJ, Compans RW, et al. Virus-like particles containing multiple M2 extracellular domains confer improved cross-protection against various subtypes of influenza virus. Mol Ther 2013; 21: 485–92. [PubMed: 23247101]
6. Wang Y, Deng L, Gonzalez GX, Luthra L, Dong C, Ma Y, et al. Double-Layered M2e-NA Protein Nanoparticle Immunization Induces Broad Cross-Protection against Different Influenza Viruses in Mice. Adv Healthcare Mater 2020; 9: e1901176.
7. Wang Y, Li S, Dong C, Ma Y, Song Y, Zhu W, et al. Skin vaccination with dissolvable microneedle patches incorporating influenza neuraminidase and flagellin protein nanoparticles induces broad immune protection against multiple influenza viruses. ACS Appl Bio Mater 2021; 4: 4953–61.
8. Deng L, Chang TZ, Wang Y, Li S, Wang S, Matsuyama S, et al. Heterosubtypic influenza protection elicited by double-layered polypeptide nanoparticles in mice. Proc Natl Acad Sci U S A. 2018; 115: E7758–E67. [PubMed: 30065113]
9. Westgeest KB, Russell CA, Lin X, Spronken MI, Bestebroer TM, Bahl J, et al. Genomewide analysis of reassortment and evolution of human influenza A(H3N2) viruses circulating between 1968 and 2011. Journal of virology. 2014; 88: 2844–57. [PubMed: 24371052]
10. Kilbourne ED, Johansson BE, Grajower B. Independent and disparate evolution in nature of influenza A virus hemagglutinin and neuraminidase glycoproteins. Proc Natl Acad Sci U S A. 1990; 87: 786–90. [PubMed: 2300562]
11. Doyle TM, Hashem AM, Li C, Van Domselaar G, Larocque L, Wang J, et al. Universal anti-neuraminidase antibody inhibiting all influenza A subtypes. Antiviral research. 2013; 100: 567–74. [PubMed: 24091204]
12. Kim KH, Jung YJ, Lee Y, Park BR, Oh J, Lee YN, et al. Cross protection by inactivated recombinant influenza viruses containing chimeric hemagglutinin conjugates with a conserved neuraminidase or M2 ectodomain epitope. Virology. 2020; 550: 51–60. [PubMed: 32882637]
13. Sei CJ, Rao M, Schuman RF, Daum LT, Matyas GR, Rikhi N, et al. Conserved Influenza Hemagglutinin, Neuraminidase and Matrix Peptides Adjuvanted with ALFQ Induce Broadly Neutralizing Antibodies. Vaccines. 2021; 9.

14. Bullard BL, Weaver EA. Strategies Targeting Hemagglutinin as a Universal Influenza Vaccine. Vaccines. 2021; 9: 257. [PubMed: 33805749]
15. Hu Y, Sneyd H, Dekant R, Wang J. Influenza A Virus Nucleoprotein: A Highly Conserved Multi-Functional Viral Protein as a Hot Antiviral Drug Target. Current topics in medicinal chemistry. 2017; 17: 2271–85. [PubMed: 28240183]
16. Deliyannis G, Jackson DC, Ede NJ, Zeng W, Hourdakis I, Sakabetis E, et al. Induction of long-term memory CD8(+) T cells for recall of viral clearing responses against influenza virus. Journal of virology. 2002; 76: 4212–21. [PubMed: 11932386]
17. Irvine DJ, Swartz MA, Szeto GL. Engineering synthetic vaccines using cues from natural immunity. Nat Mater 2013; 12: 978–90. [PubMed: 24150416]
18. Lopez-Sagaseta J, Malito E, Rappuoli R, Bottomley MJ. Self-assembling protein nanoparticles in the design of vaccines. Comput Struct Biotechnol J 2016; 14: 58–68. [PubMed: 26862374]
19. Dong CH, Wang Y, Zhu WD, Ma Y, Kim J, Wei L, et al. Polycationic HA/CpG Nanoparticles Induce Cross-Protective Influenza Immunity in Mice. ACS Appl Mater Interfaces. 2022; 14: 6331–42. [PubMed: 35084819]
20. Chang TZ, Deng L, Wang BZ, Champion JA. H7 Hemagglutinin nanoparticles retain immunogenicity after >3 months of 25 degrees C storage. PloS one. 2018; 13: e0202300.
21. Dong C, Wang B-Z. Engineered Nanoparticulate Vaccines to Combat Recurring and Pandemic Influenza Threats. Advanced NanoBiomed Research. 2022; 2: 2100122.
22. Ma Y, Wang Y, Dong C, Gonzalez GX, Song Y, Zhu W, et al. Influenza NP core and HA or M2e shell double-layered protein nanoparticles induce broad protection against divergent influenza A viruses. Nanomedicine. 2022; 40: 102479.
23. Wang Y, Deng L, Kang SM, Wang BZ. Universal influenza vaccines: from viruses to nanoparticles. Expert Rev Vaccines. 2018; 17: 967–76. [PubMed: 30365905]
24. Awate S, Babiuk LA, Mutwiri G. Mechanisms of action of adjuvants. Front Immunol 2013; 4: 114. [PubMed: 23720661]
25. Pulendran B, SA P, O'Hagan DT. Emerging concepts in the science of vaccine adjuvants. Nat Rev Drug Discovery. 2021; 20: 454–75. [PubMed: 33824489]
26. Johnson RS, Her GR, Grabarek J, Hawiger J, Reinhold VN. Structural characterization of monophosphoryl lipid A homologs obtained from Salmonella minnesota Re595 lipopolysaccharide. The Journal of biological chemistry. 1990; 265: 8108–16. [PubMed: 2335519]
27. Casella CR, Mitchell TC. Putting endotoxin to work for us: Monophosphoryl lipid A as a safe and effective vaccine adjuvant. Cell Mol Life Sci 2008; 65: 3231–40. [PubMed: 18668203]
28. Kamphuis T, Meijerhof T, Stegmann T, Lederhofer J, Wilschut J, de Haan A. Immunogenicity and protective capacity of a virosomal respiratory syncytial virus vaccine adjuvanted with monophosphoryl lipid A in mice. PloS one. 2012; 7: e36812. [PubMed: 22590614]
29. Zhu WD, Dong CH, Wei L, Wang BZ. Promising Adjuvants and Platforms for Influenza Vaccine Development. Pharmaceutics. 2021; 13.
30. Del Giudice G, Rappuoli R, Didierlaurent AM. Correlates of adjuvanticity: A review on adjuvants in licensed vaccines. Semin Immunol 2018; 39: 14–21. [PubMed: 29801750]
31. Dong W, Bhide Y, Marsman S, Holtrop M, Meijerhof T, de Vries-Idema J, et al. Monophosphoryl Lipid A-Adjuvanted Virosomes with Ni-Chelating Lipids for Attachment of Conserved Viral Proteins as Cross-Protective Influenza Vaccine. Biotechnology journal. 2018; 13: e1700645.
32. Rhee EG, Kelley RP, Agarwal I, Lynch DM, La Porte A, Simmons NL, et al. TLR4 ligands augment antigen-specific CD8+ T lymphocyte responses elicited by a viral vaccine vector. J Virol 2010; 84: 10413–9. [PubMed: 20631129]
33. Chen C, Zhang CG, Li RM, Wang ZM, Yuan YM, Li HQ, et al. Monophosphoryl-Lipid A (MPLA) is an Efficacious Adjuvant for Inactivated Rabies Vaccines. Viruses-Basel. 2019; 11.
34. Lawson CM, Bennink JR, Restifo NP, Yewdell JW, Murphy BR. Primary pulmonary cytotoxic T lymphocytes induced by immunization with a vaccinia virus recombinant expressing influenza A virus nucleoprotein peptide do not protect mice against challenge. Journal of virology. 1994; 68: 3505–11. [PubMed: 7514677]
35. Krammer F, Smith GJD, Fouchier RAM, Peiris M, Kedzierska K, Doherty PC, et al. Influenza. Nature reviews Disease primers. 2018; 4: 3.

36. Bouvier NM, Palese P. The biology of influenza viruses. Vaccine. 2008; 26 Suppl 4: D49–53. [PubMed: 19230160]
37. Deng L, Wang BZ. A Perspective on Nanoparticle Universal Influenza Vaccines. ACS Infect Dis 2018; 4: 1656–65. [PubMed: 30394725]
38. Weber C, Coester C, Kreuter J, Langer K. Desolvation process and surface characterisation of protein nanoparticles. International journal of pharmaceutics. 2000; 194: 91–102. [PubMed: 10601688]
39. Verma D, Gulati N, Kaul S, Mukherjee S, Nagaich U. Protein Based Nanostructures for Drug Delivery. Journal of pharmaceutics. 2018; 2018: 9285854.
40. Storp B, Engel A, Boeker A, Ploeger M, Langer K. Albumin nanoparticles with predictable size by desolvation procedure. Journal of microencapsulation. 2012; 29: 138–46. [PubMed: 22329480]
41. Deng L, Kim JR, Chang TZ, Zhang H, Mohan T, Champion JA, et al. Protein nanoparticle vaccine based on flagellin carrier fused to influenza conserved epitopes confers full protection against influenza A virus challenge. Virology. 2017; 509: 82–9. [PubMed: 28622575]
42. Jazayeri SD, Poh CL. Development of Universal Influenza Vaccines Targeting Conserved Viral Proteins. Vaccines. 2019; 7.
43. Huber VC, McKeon RM, Brackin MN, Miller LA, Keating R, Brown SA, et al. Distinct contributions of vaccine-induced immunoglobulin G1 (IgG1) and IgG2a antibodies to protective immunity against influenza. Clin Vaccine Immunol 2006; 13: 981–90. [PubMed: 16960108]
44. Kopf M, Le Gros G, Bachmann M, Lamers MC, Bluethmann H, Kohler G. Disruption of the murine IL-4 gene blocks Th2 cytokine responses. Nature. 1993; 362: 245–8. [PubMed: 8384701]
45. Miyauchi K, Adachi Y, Tonouchi K, Yajima T, Harada Y, Fukuyama H, et al. Influenza virus infection expands the breadth of antibody responses through IL-4 signalling in B cells. Nat Commun 2021; 12.
46. Bot A, Bot S, Bona CA. Protective role of gamma interferon during the recall response to influenza virus. J Virol 1998; 72: 6637–45. [PubMed: 9658110]
47. Yin Y, Li B, Zhou L, Luo J, Liu X, Wang S, et al. Protein transduction domain-mediated influenza NP subunit vaccine generates a potent immune response and protection against influenza virus in mice. Emerg Microbes Infect 2020; 9: 1933–42. [PubMed: 32811334]
48. Withanage K, De Coster I, Cools N, Viviani S, Tourneur J, Chevandier M, et al. Phase 1 Randomized, Placebo-Controlled, Dose-Escalating Study to Evaluate OVX836, a Nucleoprotein-Based Influenza Vaccine: Intramuscular Results. J Infect Dis 2022; 226: 119–27. [PubMed: 34653245]
49. Dong C, Wang Y, Gonzalez GX, Ma Y, Song Y, Wang S, et al. Intranasal vaccination with influenza HA/GO-PEI nanoparticles provides immune protection against homo- and heterologous strains. Proc Natl Acad Sci U S A. 2021; 118: e2024998118.
50. Zhu W, Pewin W, Wang C, Luo Y, Gonzalez GX, Mohan T, et al. A boosting skin vaccination with dissolving microneedle patch encapsulating M2e vaccine broadens the protective efficacy of conventional influenza vaccines. J Control Release. 2017; 261: 1–9. [PubMed: 28642154]

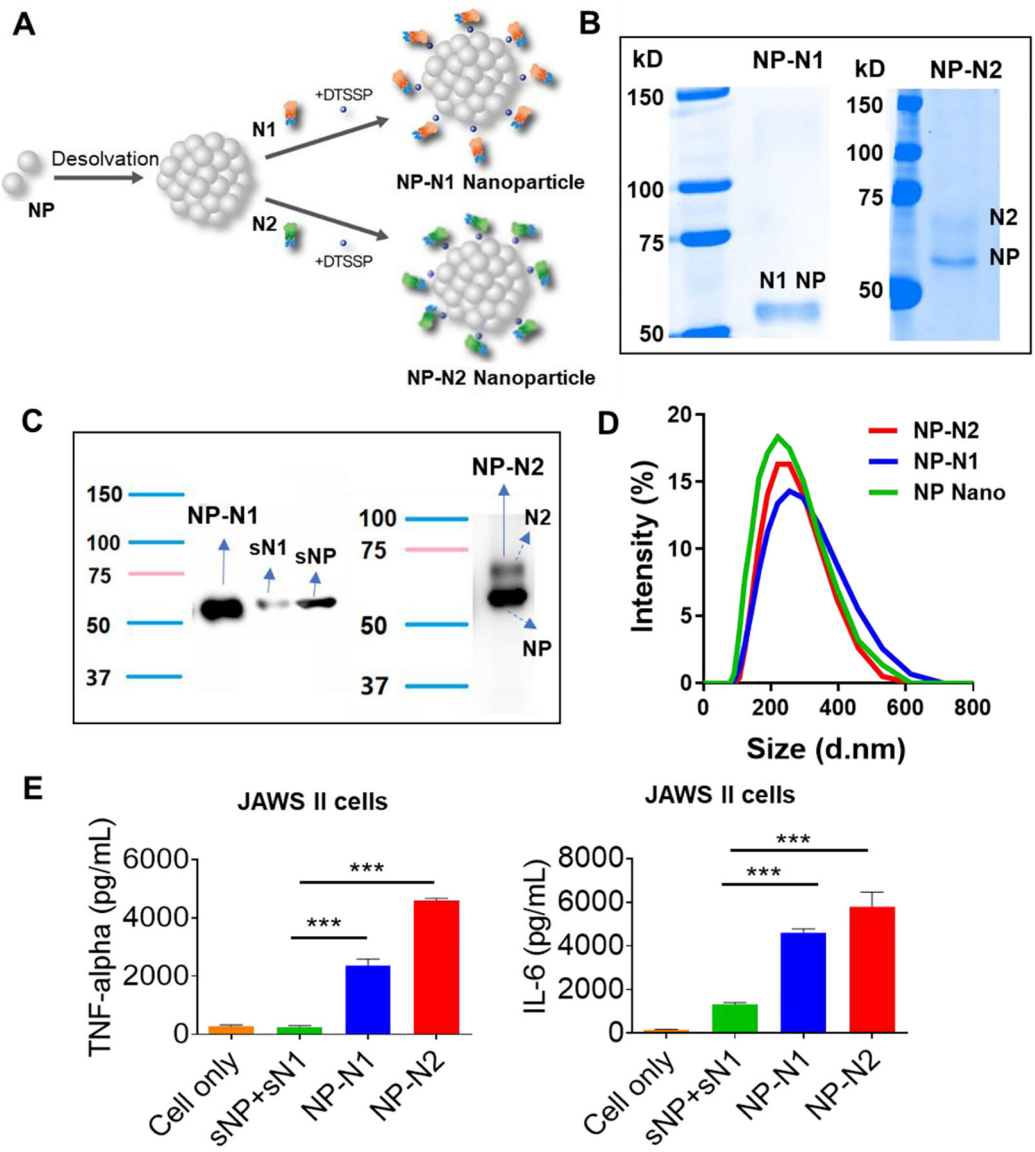

Figure 1. Characterization of NP-N1 and NP-N2 nanoparticles.

A. Diagram of layered NP-NA nanoparticle generation. NP protein nanoparticles (NP nano) were generated by ethanol desolvation. Double-layered NP-NA protein nanoparticles were formed by crosslinking NA proteins onto the surfaces of the NP particle cores. **B, C.** Coomassie blue staining and Western Blotting analysis of NP-NA nanoparticles with anti-6×His-tag antibodies. Soluble N1 and NP (sN1 and sNP) were used as controls for NP-N1 Western Blotting analysis. NP and N1 showed a similar migration in the SDS-PAGE gel. **D.** Size distribution of protein nanoparticles. **E**. Cytokines (IL-6 and TNF-α) secretion in JAWS II cells treated with sNP + sN1, NP-N1, and NP-N2 at a concentration of 5 μg/mL. (n = 3; **p < 0.01; ***p < 0.001; ns, p > 0.05)

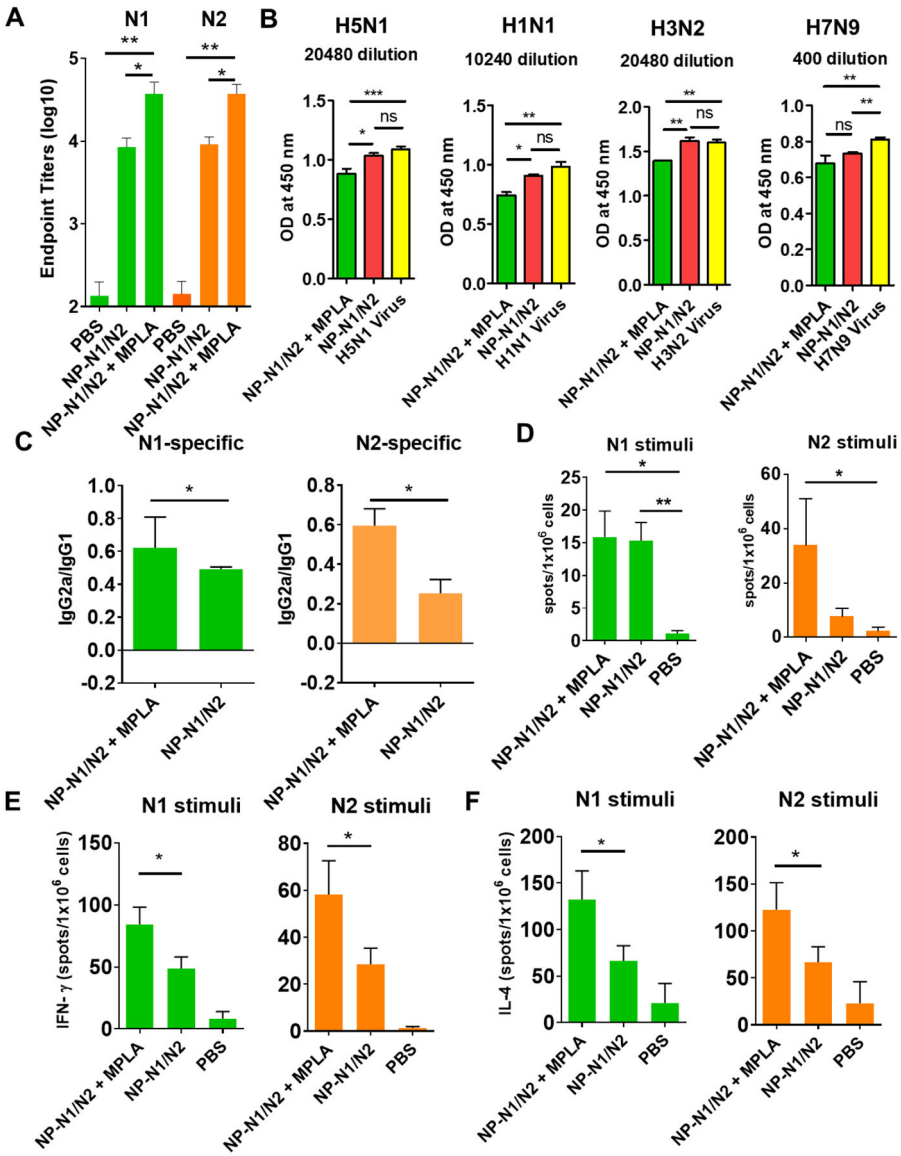

Figure 2. NA-specific humoral and cellular immune responses in vaccinated mice.

A. NA-specific antibody endpoint titers determined by ELISA. B. NAI test results against different influenza virus strains. The OD_{450} values were compared with the virus only. C. Antibody subtype IgG2a/IgG1 ratio analysis. D. NA-specific antibody-secreting cells in the bone marrow. **E-F,** NA-specific IFN-γ or IL-4 secreting splenocytes. (n = 5; * $p<0.05$; ** $p < 0.01$; *** $p < 0.001$; ns, $p > 0.05$)

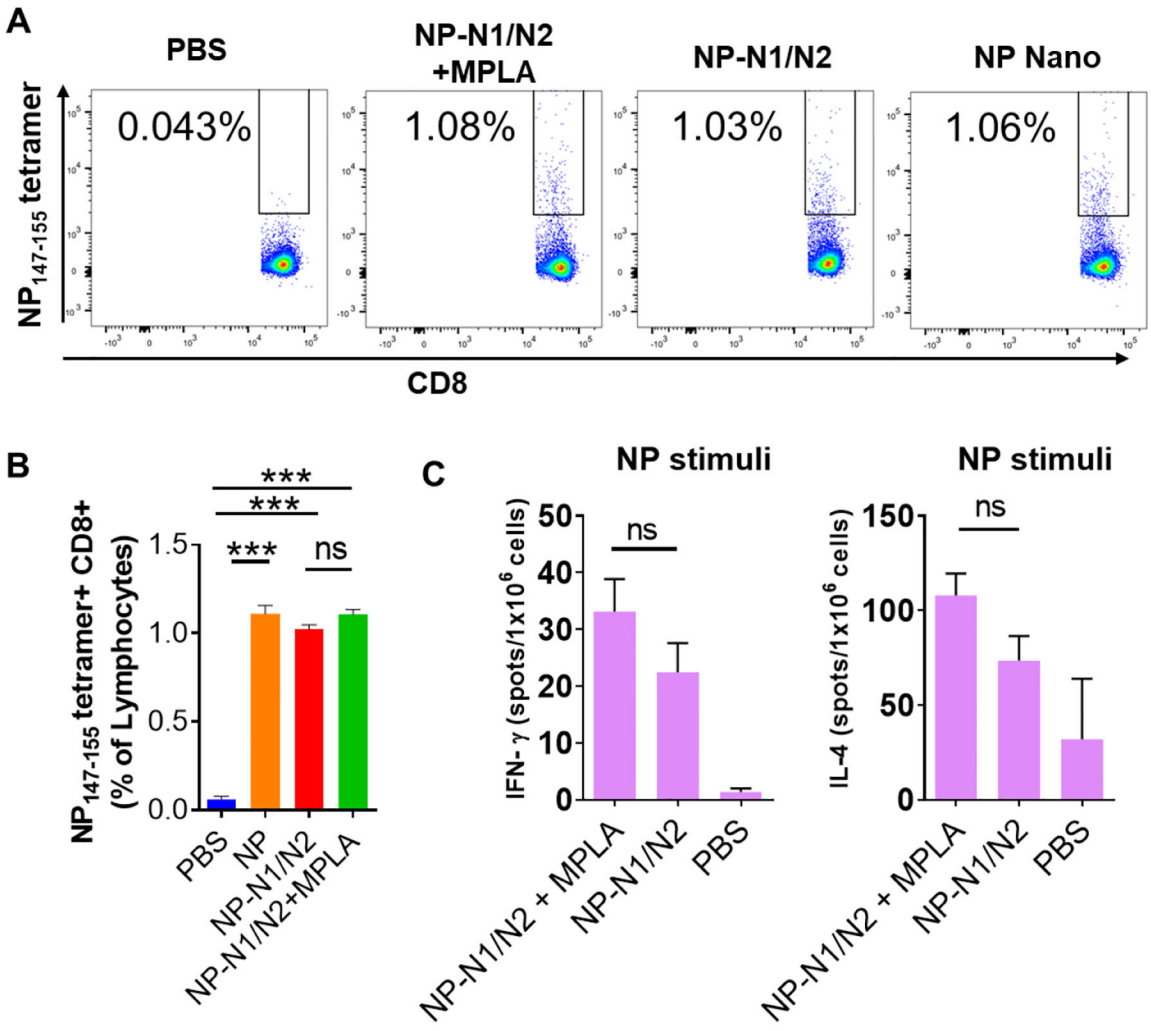

Figure 3. NP-specific cellular immune responses in vaccinated mice.

A, B The percentage of $NP_{147–155}$ tetramer^{+}CD8^{+} splenocytes post-boosting immunization. (n = 3; ***p < 0.001; ns, p > 0.05) **C.** Enumeration of NP activated IFN-γ or IL-4 secreting splenocytes by ELISpot. (n = 3; * p<0.05; ns, p > 0.05)

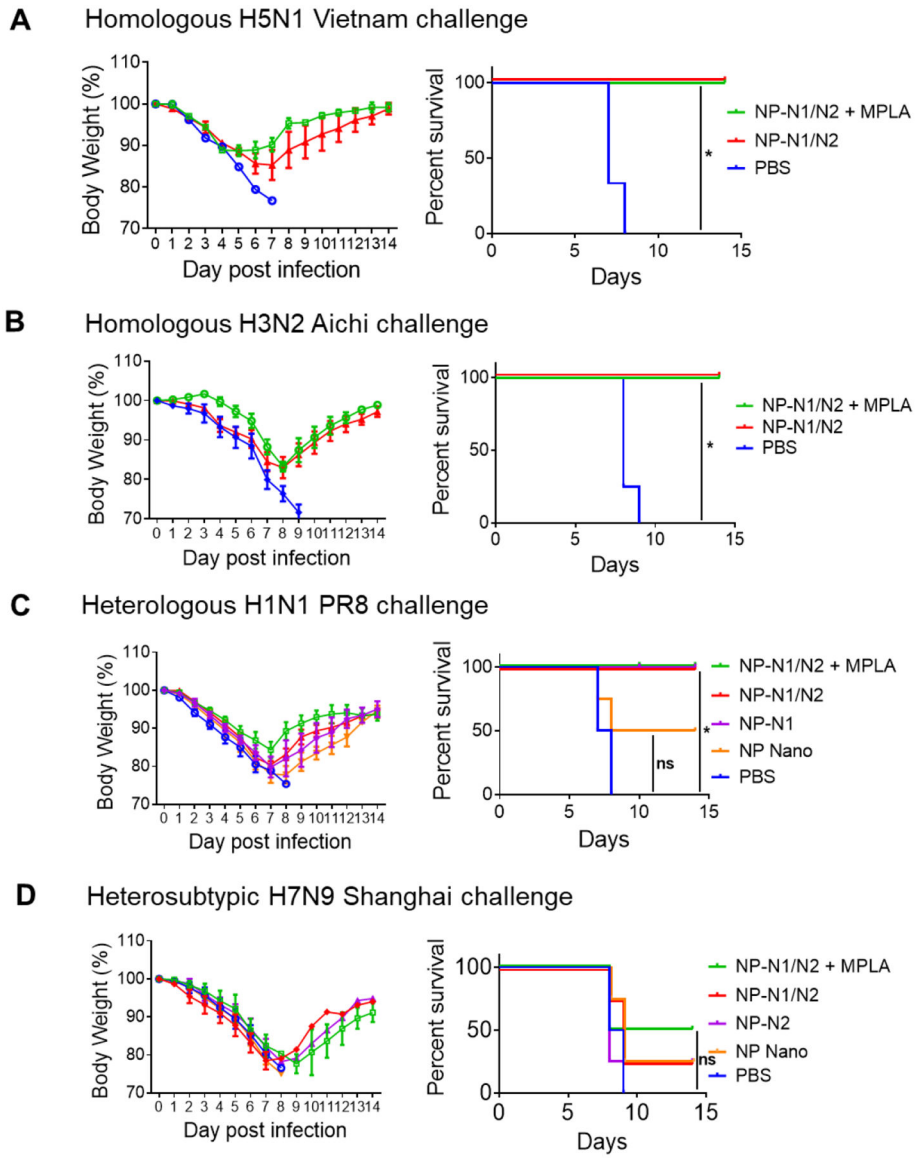

Figure 4. Immune protection against influenza viruses of homologous, heterologous, and heterosubtypic NA.

A, B. Bodyweight monitoring and survival rate post homologous NA virus challenge. Challenge dose: **A.** 5×LD_{50} rViet (H5N1); **B.** 5×LD_{50} Aichi (H3N2). **C, D.** Bodyweight monitoring and survival rate post heterologous and heterosubtypic NA virus challenge. Challenge dose: **C.**3×LD_{50} PR8 (H1N1). **D**. 3×LD_{50} Shanghai (H7N9). (*$p<0.05$, ns, no significance; n=5 for A-B; n=4 for C-D).

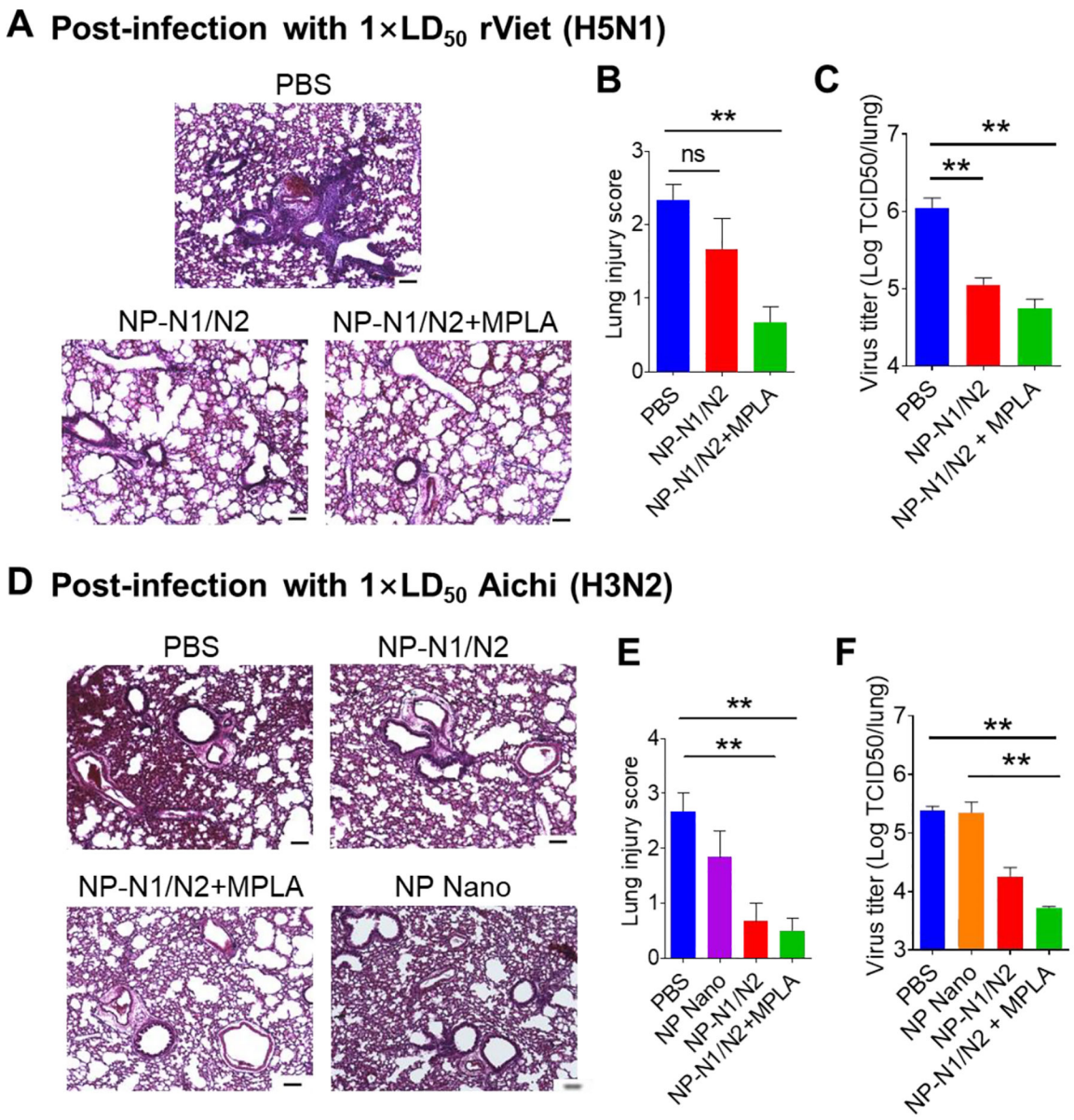

Figure 5. Histology examination and lung viral titers post virus infection.

(A, D) Histology examination by H&E staining. (B, E) Lung injury scores post-infection. (C, F) Lung virus titers post-infection. Challenge dose: A-C. 1×LD50 rViet (H5N1); D-F. 1×LD50 Aichi (H3N2). The scale bars represent 100 μm in Figures 5A and 5D. (n = 5; * $p<0.05$; ** $p < 0.01$; *** $p < 0.001$)

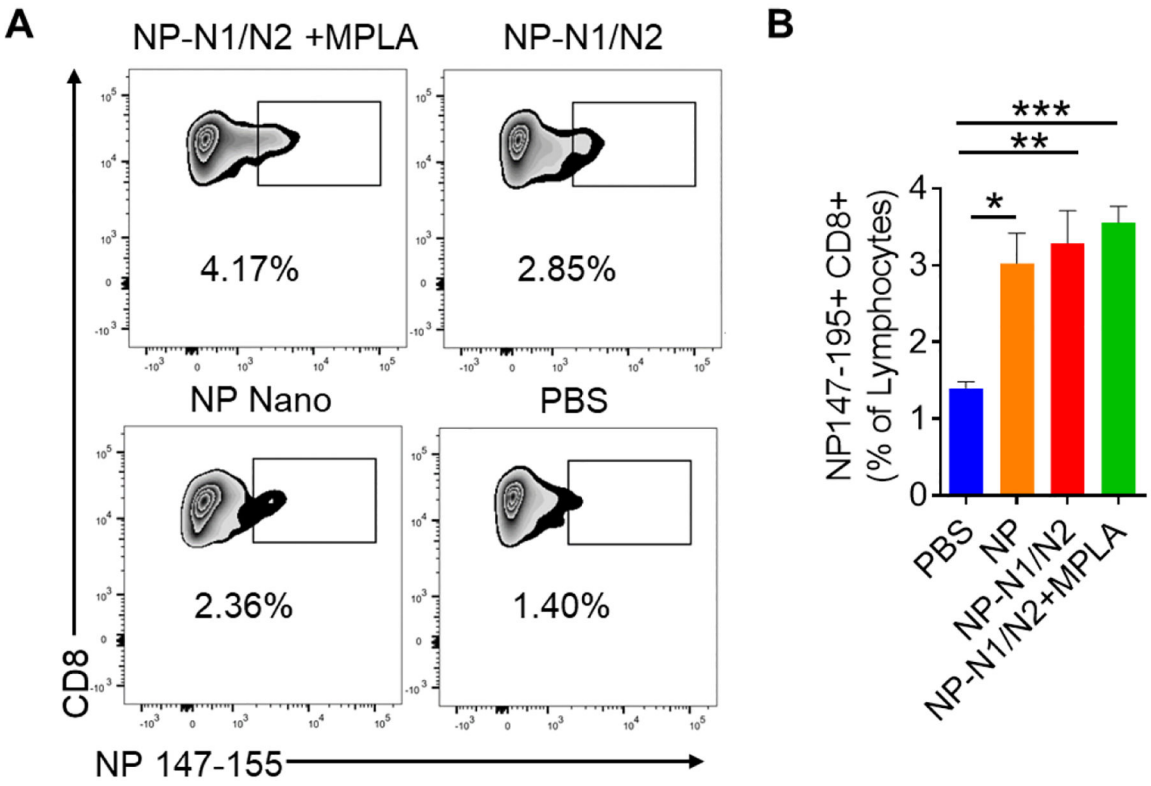

Figure 6. The NP-specific immune responses post-infection.

A. B. The percentage of $NP_{147–155}$ tetramer $^{+}CD8^{+}$ cells from the draining MLN post-infection. (n = 3; * $p<0.05$; ** $p < 0.01$; *** $p < 0.001$; ns, $p > 0.05$)